Contents lists available at Egyptian Knowledge Bank

Labyrinth: Fayoum Journal of Science and Interdisciplinary Studies

Journal homepage: https://lfjsis.journals.ekb.eg/

Multi-Classification Model for Distinguishing Covid-19 from Different Lung Diseases Based on Deep Learning Algorithms

Mohammed Abdelmoneim Alsalamony [a,*], Ahmed Salama Ismail [a], Hazem Mokhtar Elbakry [b]

[a] Department of Information Systems, Faculty of Computers and Artificial Intelligence, Fayoum University, El Fayoum 63514, Egypt
[b] Department of Information Systems, Faculty of Computers and Information Mansoura University, El-Mansoura 35516, El-Dakahleya, Egypt

ARTICLE INFO

Keywords:
Lithium-ion
batteries $Li_{1.3}Nb_{0.3}Mn_{0.4}O_2$
Thermal Analyses
Dielectric Properties

ABSTRACT

The Corona-Virus is a worldwide pandemic classified as one of the scariest viruses, according to the World Health Organization (WHO). That is because of its effect on the person's lungs, which causes high deaths. Among the vital effectiveness indicators for identifying some diseases, including the coronavirus, are computerized tomography (CT) scans and chest X-rays. Data heterogeneity between X-ray and CT biomarkers makes the learning capability of the models more challenging. Furthermore, they utilize multistage for diagnosing COVID-19 from some lung diseases. Hence, the proposed solution behind this research is to leverage form deep learning architecture for applying many classification models to resolve these problems using a fusion of two images that can identify COVID-19, pneumonia, and lung cancer in a single learning procedure. Firstly, patches are extracted from multimodal images by learning every patch using a convolutional neural network (CNN) to address these issues. Then, the available multimodal features are combined for further learning using the AlexNet classifier, the CNN classifier, and the Deep Feature Concatenation (DFC) mechanism. All the learned features are combined using a straightforward CNN. Finally, the experimental results demonstrated that the proposed AlexNet + DFC + CNN exceeded comparable work already done with 98.47 % accuracy.

1. Introduction

At the end of 2019, an ambiguous coronavirus disease began to spread globally, posing a serious threat to everyone. Eastern China's Wuhan, a town, is where the virus first appeared in December 2019. By March 2020, the (WHO) had classified the condition as a pandemic and declared it a "Public health emergency of worldwide ramifications" [1]. As of Feb 2023, the illness has impacted 673.3 million individuals worldwide, and 6.8 million deaths have been confirmed [2].

One of the most common methods for coronavirus identification is Polymerase Chain Reaction for Reverse Transcription (RT-PCR), which uses respiratory sample testing and yields results in a few hours to two days. Still, this diagnostic test is time-consuming and expensive. Accordingly, creating new viral detection techniques is still a significant issue for researchers, resulting from yet to discover a definitive medical treatment.

Prior studies have used machine learning and deep learning architecture to recognize COVID-19 in lung CT and X-ray images. For Machine learning, Yan et al. [3] aimed to create a mathematical modeling strategy based on cutting-edge interpretable machne learning algorithms, and they found the most discriminative indicators of patient survival. On the other hand, the authors of Nasiri et al. [4] used a pre-trained network, DenseNet169, was employed to extract features from X-ray images by a feature selection method, i.e., analysis of variance (ANOVA), and they classified by the eXtreme Gradient Boosting (XGBoost). In contrast, Öztürk et al. [5] developed a technique for analyzing CT and X-ray data using ML algorithms to detect viral outbreaks. Using a two-stage data augmentation approach, they also classified the images corresponding to six circumstances, including coronavirus images. Saha et al. [6] proposed a CNN architecture that detects COVID-19 in radiographs through concatenation. They constructed a multi-label algorithm to differentiate between typical standard X-ray images, viral pneumonia, and COVID-19. Bhargava et al. [7] provided an automated learning method for assessing nine datasets and identifying COVID-19. Absar et al. [8] used the SVM machine learning algorithm to obtain the COVID-19 diagnostic based on the chest radiograph pictures. In Islam et al. [9], a Contrast Limited Histogram Equalization (CLAHE) was used with CT images as a

* Corresponding author.
E-mail address: ma4240@fayoum.edu.eg (M. Alsalamony); Tel.: +201008441449

DOI: 10.21608/IFJSIS.2023.211165.1021
Received 19 May 2023; Received in revised form 04 June 2023; Accepted 21 June 2023
Available online 22 June 2023

preliminary step to enhance the image quality. Then, utilizing 2482 images of CT images in total, they created a brand-new model of a convolutional neural system that extracts 100 critical features. Following their extraction, these features were applied to a variety of methods for machine learning. Finally, they recommended an integrated approach for categorizing COVID19 Medical images. In Shan et al.[10] deployed a deep network to differentiate COVID-19-affected regions using CT images for deep understanding. In Kogilavani et al. [11], to determine COVID-19 by the employment of Lung Images, researchers have created Neural network models such as DeseNet121, NASNet, EfficientNet, and Xception. At the same time, Mishra et al. [12] examine various Deep CNN-based methods for identifying COVID-19 in chest CT images. Rehman et al. [13] proposed a deep-learning methodology using a radiograph to diagnose around 15 chest ailments. Aboughazala et al. [14] built a network to categorize Covid-19 images from radiographs as Negative or positive cases

In contrast, in Diaz-Escobar et al. [15] compared and evaluated the efficiency of different methods for finding COVID-19 pollution utilizing lung images using deep learning architectures with prior training, such as VGG19, Incep-tionV3, Xception, and ResNet50. Malik et al. [16] used a different publicly accessible benchmark database to train the Vgg-19 and CNN combo to recognize respiratory disease from chest radiographs. Rahman et al. [17] used a framework based on a deep Network and a graph of oriented variations to classify the data into More types of lung disease in addition to standard cases and find the most discriminating anomaly in anterior lung radiograph images. On the other hand, Sarkar [18] employed Vision Pro Deep Learning, a deep learning tool from COGNEX, to categorize the chest X-rays from the COVIDx dataset. Vision Pro DL is used in various industries, including life sciences and factory automation. Saood et al. [19] Used two well-known networks of the deep network to classify data, U-NET and SegNet. SegNet is described as a network for picture segmentation, and U-NET is a tool for fragmentation in healthcare.

Furthermore, multi-class segments were employed with both networks to identify the type of chest infection and to distinguish diseased from healthy lung cells using binary components. Regarding using chest radiograph pictures in diagnosing and determining COVID-19 patients, a three-supervised learning architecture was developed by Hassantabar et al. [20], and Imani [21] created convolutional filters that decreased the contextual features. The lung X-ray and the abdomen CT scans were also used to extract shape and textural information as contextual feature maps. Additionally, even before symptoms appear, a chest CT image is beneficial. It reliably picks up the aberrant features visible in images, in contrast to how a lung X-ray is less helpful at the beginning of the condition. Combining the characteristics of these two types of images will boost classification accuracy.

Various steps have been taken to distinguish COVID-19 from other lung X-ray and CT images, and numerous deep-learning architectures have been employed. Khalifa et al. [22] provided a methodology for deep learning that combines deep transfer learning with generative adversarial networks (GAN). Additionally, they used GAN to increase the sample size for deep transfer model training. Additionally, they used the models for deep transfer learning AlexNet and GoogleNet to determine pneumonia from lung X-rays. On the other hand, in Ibrahim et al. [23], a combination of X-ray and CT images was used to train a multi-classification model to detect lung cancer, pneumonia, and COVID-19. Moreover, they expanded the dataset by linking lung X-rays and CT images, which raised classification accuracy. Besides, while training the model, they considered four distinct deep learning architectures.

Although methods in the literature achieved promising performance, they still have some limitations.

The first restriction in these articles [11, 17, 18, 20, 22] is that they seldom considered the heterogeneity between various imaging techniques [5, 21, 23]; To diagnose lung disorders, they used chest X-rays or CT scans independently. To get around the issue mentioned earlier, the learning process combines CT and X-ray scans, which uses two different types of imaging.

The second restriction identified in these studies [5, 13, 19, 20] is that the models were trained in two stages. They used various augmentation techniques to enhance the amount of deep learning method samples in the initial stage. Additionally, they trained the deep-learning models in the second stage using the original and enhanced photos. A deep learning architecture that can recognize COVID-19 in a single learning operation was used to resolve the mentioned issue.

The third kind of restriction found in these studies [10, 11, 19] is that they are usually diagnosed with two different kinds of lung diseases. However, numerous lung ailments exist, like Lung cancer and COVID-19. To overcome the mentioned issue, utilizing deep learning architecture help to diagnose many lung diseases using a combination of lung X-ray and CT images.

This research proposes a new multimodal for distinguishing COVID-19 from lung cancer and pneumonia in one learning process, which includes X-ray and CT. Firstly, extract 2D patches from multimodal images, and meanwhile, learn every patch using a CNN. Then, the available multimodal features are combined for further learning using CNN. Finally, combining all the features discovered leads to the diagnosis of lung diseases. As a finding of the analysis, the following significant contributions were made: First, a unique paradigm for using multimodal data was suggested, including X-ray and CT images, for classification in a single learning procedure. It differs significantly from earlier research that separately teaches each modality before using a deep CNN. Second, to reduce data heterogeneity, one CNN is applied to each patch, then integrating the final features for classification.

The research is structured into sections: Section 2, Materials, Procedures, study dataset, data preparation, and suggested deep learning framework are discussed in detail. In section 3, the proposed experiments delivered from the deep learning approach are described and evaluated. In Section 4, significant findings and results are presented. Finally, a conclusion and future contributions are illustrated in Section 5.

2. Proposed Methodology

The proposed model for employing the Alexnet CNN architecture to identify some lung diseases is shown in Fig. 1. This suggested model aims to classify a given CT and X-ray images into COVID-19, normal, pneumonia, or lung cancer categories in a single learning process that is divided into five crucial phases: pre-processing (normalization, patching, and resizing), feature extraction, DFC, fully connected layer, and classification using pre-trained CNN architectures. The following sub-sections go into more detail with each stage's description.

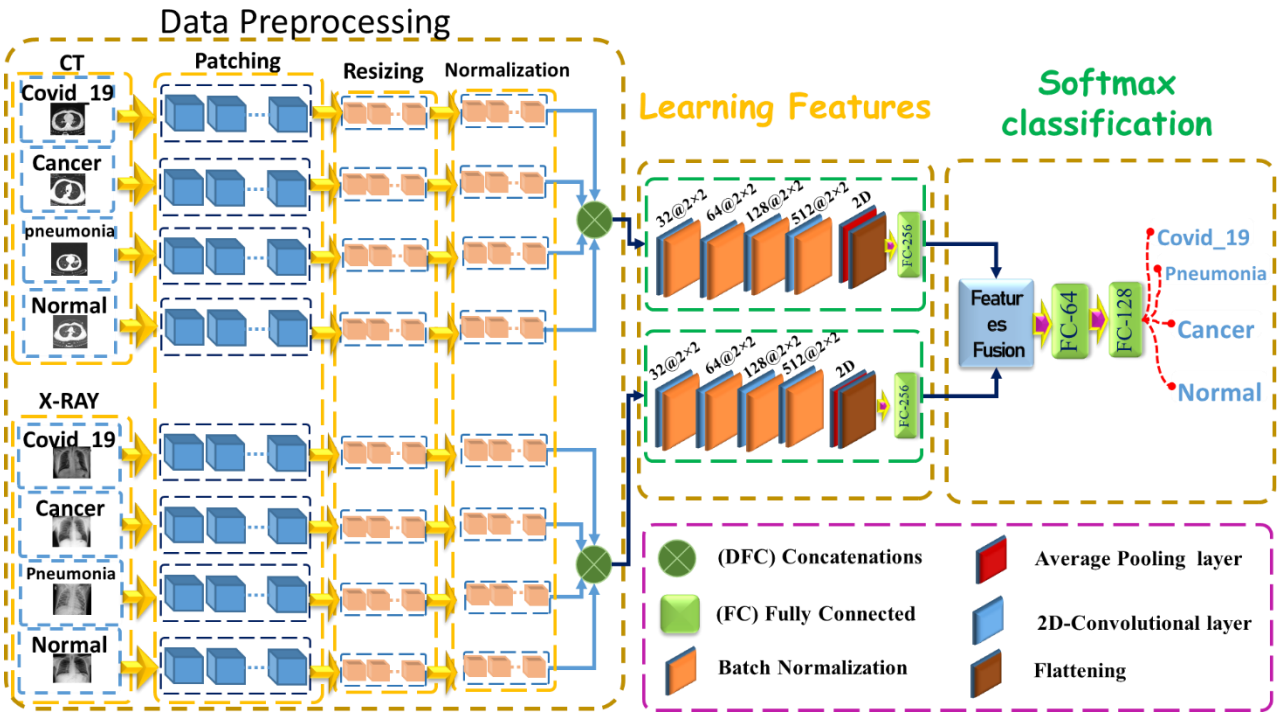

Fig.1. Summary of the suggested COVID-19, pneumonia, and lung cancer detection approach using CNN.

2.1. Data Pre-processing

The techniques employed during the pre-processing stage are thoroughly described in this section: Data normalization is an important step to ensure numerical stability in CNN systems. Gradient descent is more likely to be stable with normalization and learn quickly with a CNN model. Therefore, the input images' pixel values were adjusted for this investigation to fall between 0 and 1, rescaled by multiplying the pixel values by 1/255. The grayscale images were used in the datasets under consideration because it was found that the pre-trained models on gray images outperformed the models that were trained in color images in terms of speed and accuracy [24]. In addition, there are some colored images within the set of images used in the proposed form. The CT and X-ray pictures obtained from various sources were acquired and combined for the studies. This collection comprises images that show COVID-19, lung cancer, and pneumonia. Firstly, we chose a dataset for COVID-19 made up of approximately 4320 images from repositories like GitHub [25, 26]. Secondly, certain helpful websites, including Radiopaedia, Medical and Interventional Radiology in Italy (SIRM), and the Radiological Society of North America (RSNA), offer public and custom data sets, of which datasets are recognized to be the most popular. These 5856 images represent a compilation of common pneumonia X-ray images [27, 28] to train the proposed deep CNN model to distinguish between pneumonia and COVID-19 and utilize this data. In addition, a user of the public Standard Digital Image Database collected by the Japanese Society of Radiological Technology (JSRT). An extensive collection of annotated photos, including around 20,000 images of lung cancer, are available for research, training, and education through the JSRT database [29, 30]. X-ray and CT images totaling 3500 that make up the final dataset for this investigation are referred to as "standard images. "From the datasets that were gathered, 6577 images in total were chosen. The images that were collected from freely accessible resources had varying resolution sizes. The previous references utilized images in the proposed model, displayed in Table 1. Pre-processing images are changed in size to 128×128×1 to unify the size of the images because the images used in the model have different dimensions in addition to absorbing resources from the RAM space and storage capacity of the images used. Image patches are extracted randomly from CT and X-ray images with 100 × 100 window size.

Table 1: A short description of the class names, modality, and number of images included in datasets for the use of CT and X-ray images in training and validation procedures

Class name	*Data Source*	*Modality*	*number of used images*
Normal	*[31]*	*X-ray*	*1000*
Normal	*[32]*	*CT*	*1000*
Covid-19	*[31]*	*X-ray*	*1000*
Covid-19	*[32]*	*CT*	*1000*
Pneumonia	*[31]*	*X-ray*	*1000*
Pneumonia	*[32]*	*CT*	*1000*
Cancer	*[33]*	*X-ray*	*247*
Cancer	*[29]*	*CT*	*330*

Due to the memory space, storage space, and the power of the processing, not all the images collected from different sources were used to be an input in the proposed learning model. Table 1 shows the number of images used in the proposed learning model.

2.2. Learning Features

To turn the local chest picture into more compact high-level features of images, as shown in Fig. 1, a cascaded Alexnet CNNs was built to learn the multimodal features of lung X-ray and CT image patches.

2.2.1. AlexNet Architecture

Alexnet CNNs deep learning architecture in the outlined work used for each Image class. (One for X-ray and the other for CT), the elements of the architecture explained in Fig.2.

Five convolutional layers with rectified linear units and three max-pooling layers are used in the suggested system. In the first layer, the filter is 96, and the kernel size is 11×11 with stride 4. In the second layer, the filter is 256, and the kernel size is 5 × 5. In the third and fourth layers, the filter is 384, and the kernel size is 3 × 3. The filter for the fifth convolutional layer is 256 kernels of size 3 × 3. A feature map is produced for each convolutional layer. The first, second, and fifth layers' feature maps are combined with the pooling layers of 3 × 3 and stride of 2 × 2. The system has 100 nodes and eight layered architectures. This produces trainable feature maps, meaning feature extraction processes occur at these levels. Fully connected layers (FC) are utilized to place these feature maps and use Softmax activation to calculate the classification's possibilities. The dataset only has four classes, although the Soft-max layer's type can provide courses with up to 1000 various classes.

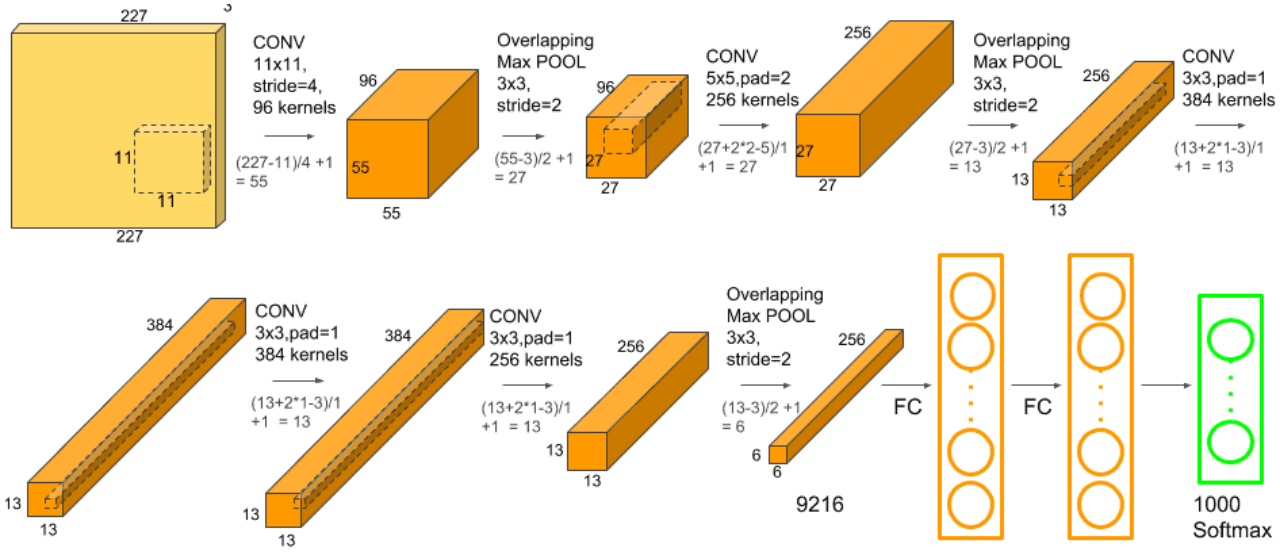

Fig.2. AlexNet convolution neural network architecture [34]

2.2.2. Convolution Layer

This layer generates the feature maps shown as the input to classification layers. It includes a kernel to create the feature map as the output. A matrix multiplication and result integration at every point on the input is executed. The definition of the generated feature map is as follows:

$$N_x^r = \frac{N_x^{r-1} - L_x^r}{S_x^r} + 1 \; ; N_y^r = \frac{N_y^{r-1} - L_y^r}{S_y^r} + 1 \qquad (1) \quad [35]$$

Where (N_x, N_y) is the width and height of the output feature map of the last layer and (L_x, L_y) is the kernel size, (S_x, S_y) that defines the number of pixels skipped by the kernel in horizontal and vertical directions and index r indicates the layer, i.e., $r = 1$. Convolution is applied on the input feature map and a kernel to get the output feature map that is defined as:

$$X_1(m.n) = (J * R)(m.n) \qquad (2) \quad [35]$$

$X_1 (m, n)$ expresses a feature map with two dimensions, m and n. R is the kernel of size (L_x, L_y) and feature map input J. To illustrate the convolution between J and R, use *. Convolution is expressed as the following:

$$X_1(m.n) = \sum_{p=-\frac{L_x}{2}}^{p=+\frac{L_x}{2}} \sum_{q=-\frac{L_y}{2}}^{q=+\frac{L_y}{2}} J(m-p.n-q)R(p.q) \qquad (3) \quad [35]$$

In the suggested framework, five CONV layers with a RELU layer are used to accurately train the dataset and extract the most feature maps possible from the input frames.

2.2.3. Rectified Linear Unit Layer

A RELU activation function makes the proposed network non-linear and applies to all the trainable layers. This layer appropriately considers the nonlinearities and is utilized with the final feature map generated by the convolutional layer. The non-linear gradient descent is covered using tanh (.) and the RELU activation function. Tanh (.) is expressed as:

$$X_2(m.n) = tanh\big(X_1(m.n)\big) = \frac{sinh(X_1(m.n))}{cosh(X_1(m.n))} = 1 + \frac{1-e^{-2*X_1(m.n)}}{1+e^{-2*X_1(m.n)}} \quad (4) \quad [35]$$

Where $X_2(m, n)$ is a two-dimensional output feature map after applying tanh(.) on the input feature map $X_1(m, n)$, which is achieved after passing through the convolutional layer.

The values in the final feature map are obtained after applying the RELU function as follows:

$$X(m.n) = \begin{cases} 0. & if X_2(m.n < 0) \\ X_2(m.n). & if X_2(m.n \geq 0) \end{cases} \quad (5) \quad [35]$$

In *eq. (5), X (m, n)* is produced by turning the negative numbers into zero, and it returns the same result when it receives a positive value. The RELU layer speeds the training of deep convolutional neural networks.

2.2.4. Maximum Pooling Layer

The suggested architecture includes a pooling layer after the first, second, and fifth convolution layers to scale back each frame's computational expense and spatial dimension for the proposed deep learning framework. The pooling process typically selects each image slice's average or maximum value. In the suggested work, pooling is used with the maximum value against each piece because the outcomes were better in this configuration. The use of the highest pooling layer for downsampling the images on the activation output is illustrated in Fig. 3.

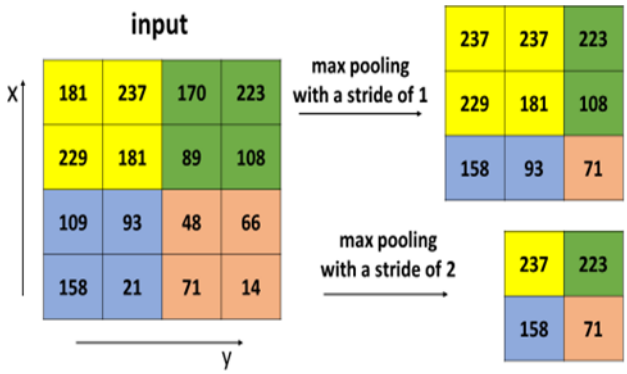

Fig.3. Maximum pooling layer [36]

2.2.5. Dropout Layer

The first two wholly connected layers employ the dropout layer to prevent overfitting of the data. It uses neural networks to average models and is a very effective method for regularising training data. They used the highest pooling layer to generate feature maps by selecting the maximum pixel per map, convolutional layer kernel sizes, and their skipping factors. The output of the topmost layers is also linked to a 1D feature vector by a fully connected layer. The output unit for the class label must always be fully connected to the top layer for extracting the advanced training features; Fig. 4 depicts the regularization technique on thoroughly combined layers before and after applying dropout.

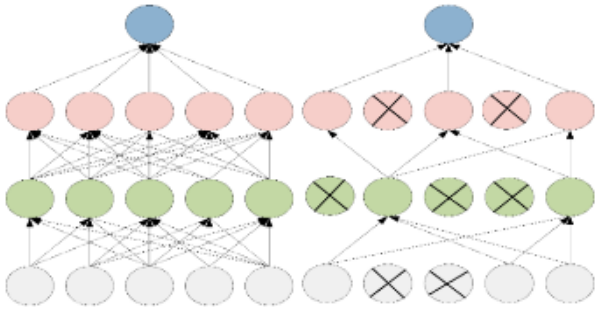

Fig.4. Fully connected layers (FC) before and after applying dropout [35]

2.3. Deep feature concatenation

Concatenating features is a valuable technique for combining many features to improve categorization. In this study, the proposed CNNs are used to extract X-ray and CT characteristics, and then the DFC is employed; as seen in Fig. 5, the classification descriptor is then formed by connecting these features:

$$\text{Final Feature Descriptor} = F^{(CT)} \cup F^{(X-ray)} \quad (6) \quad [37]$$

F (CT) denotes the features of CT images, and F (X-ray) is the features of X-ray images.

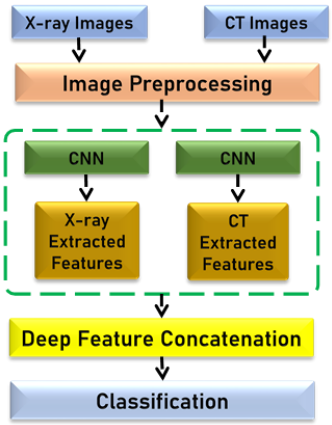

Fig. 5. Deep feature concatenation architecture [37]

2.4. Classification (SoftMax classifier)

The softmax activation function, which determines the probability for each category based on chest X-ray and CT patches, receives the output of CNN's Feature Extraction technique and DFC approach. The suggested approach can automatically learn general, multi-level, and multimodal characteristics from several imaging modalities for classification, and the final feature descriptor is used in the classification procedure to identify the type of disease, and the softmax layer calculates the scores of the classes as:

$$L_{softmax} = -\sum_{i=1}^{N} \log \frac{e^{w_{yi}^{T} f_i + b_{yi}}}{\sum_{j=1}^{k} e^{w_j^{T} f_i + b_j}} \quad (7) \quad [37]$$

Where fi denotes features and yi is the proper class label of the ith image. Wj and bj are the weights and biases of the jth class, respectively. N is the value of training samples, and K is the total count of classes.

3. Results and Discussion

the experimental results of the proposed model for categorizing the four patients illustrated in this section using lung X-rays and CT images. The proposed model's various hyperparameters, including learning rate, splits, iterations, call-backs, epochs, and batch size, were adjusted by grid search techniques. The model has been trained for 300 epochs. The batch size for the proposed model was set to 100. Accuracy, sensitivity, precision, and F1-score were used to calculate the performance of the suggested model for each class label.

3.1. Experimental parameters

The Keras framework was applied to develop the model. Python 3.8 was used to execute the models. A Kaggle cloud with 73 GB of storage, 13 GB of memory, and (15 GB) Graphics Processing Unit (GPU) type P100 to experiment. Every image was sent to the Keras Image Data Generator class for pre-processing tasks, including scaling, patching, and normalizing. The "Adaptive Moment Estimation" (Adam) optimizer was employed for the suggested model, and the model's learning rate (LR) parameter is listed as 0.001 throughout the entire code.

3.2. Performance indicators

Several metrics, inclusive accuracy (ACC), positive predictive value, also known as precision, specificity (SPC), sensitivity (recall), and F1 score, are defined by Eqs. (8) through (12)[38] were used to assess the effectiveness of the chest illness classification model.

Where *TP* refers to the true positive, *TN* refers to the negative parameters. *FP* refers to the false positive, and *FN* refers to the false negative values. Accuracy, given in *eq. (8)* how many examples can be correctly predicted based on the number of examples?

$$Accuracy\ (ACC) = \frac{TP+TN}{TP+TN+FP+FN} \quad (8)$$

Sensitivity or recall, given in *eq. (9)*.

$$Recall\ (Sensitivity) = \frac{TP}{TP+FN} \quad (9)$$

Specificity, given in *eq. (10)*.

$$Specificity\ (SPC) = \frac{TN}{TN+FP} \quad (10)$$

eq. (11) shows precision

$$Precision\ (PPV) = \frac{TP}{TP+FP} \quad (11)$$

Finally, the F1 score is shown in eq. *(12)*

$$F1\text{- }score = \frac{Two*TP}{Two*TP+FP+FN} \quad (12)$$

3.3. Results of multi-classification deep learning model

This section presents the findings of proposed multi-classification and binary models, which depend on the confusion metrics results for various classes, as shown in Table 2.

Table 2: Results of confusion metrics for various numbers of classes (proposed model)

Classes	Image Type	ACC. (%)	SEN. (Recall)(%)	SPC. (%)	PRE.(%)	F1 –Score (%)
Covid-19 Vs. Pneumonia Vs. Cancer Vs. Normal	CT	99.93	99.95	99.97	99.95	99.95
	X-ray	97.95	97.17	99.02	97.41	97.27
	Fusion (CT+X-ray)	**98.47**	**98.44**	**99.46**	**98.54**	**98.48**
Covid-19 Vs. Pneumonia Vs. Normal	CT	98.88	99.67	98.12	98.33	98.95
	X-ray	98.05	96.59	99.49	99.46	97.98
	Fusion (CT+X-ray)	**99.16**	**99.28**	**99.03**	**99.04**	**99.16**
Covid-19 Vs. Cancer Vs. Normal	CT	99.70	99.80	99.60	99.60	99.70
	X-ray	98.13	98.09	98.18	98.22	98.14
	Fusion (CT+X-ray)	**98.72**	**98.64**	**98.79**	**98.79**	**98.72**
Covid-19 Vs. Normal	CT	99.65	99.90	99.40	99.42	99.65
	X-ray	98.20	97.40	99	98.98	98.17
	Fusion (CT+X-ray)	**99.22**	**99.25**	**99.20**	**99.20**	**99.22**

The results of the proposed model described in Table 2 used one type of image or fused the two types (fusion of X-ray and CT images) in a single learning process for lung diseases.

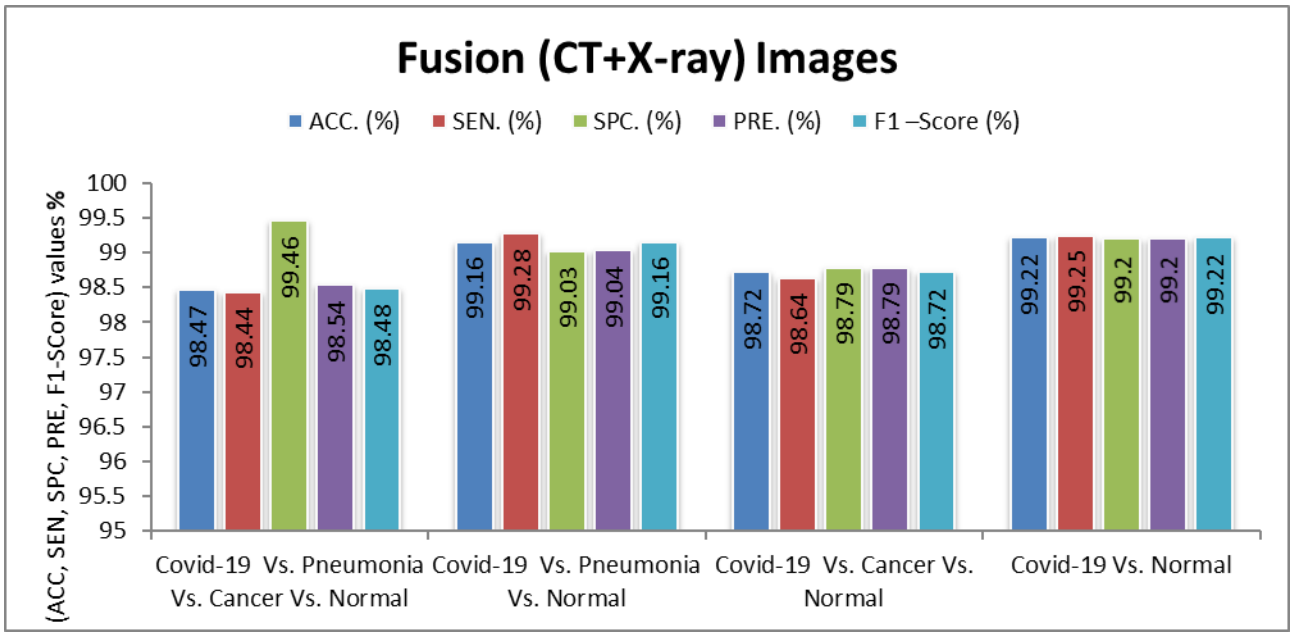

Fig. 6. Results of confusion metrics for various numbers of classes in multiple images

Findings of multi-classification and binary models seen in Fig. 6, Represented in accuracy, sensitivity, precision, specificity, and F1 score on the Y-axis, which depend on the confusion metrics results for (Covid-19, Normal), (Covid-19, Cancer, Normal), (Covid-19, Pneumonia, Normal) and (Covid-19, Pneumonia, Cancer, Normal) on X-axis in X-ray and CT images.

3.4. Discuss the suggested model with earlier studies on coronavirus classification.

This section discusses the proposed research's outcomes with previously used methods and different types of images for the classification of COVID-19 in chest X-ray images, CT images, and fusion of X-ray and CT image features. Still, they did not use the same collection of pictures with each other that was used in this research because it was collected from various previous sources and studies; however, studies whose results are discussed used parts of the image collection that was used in this research.

Table 3: Discuss the proposed model with earlier studies for COVID-19 diagnosis in pneumonia, lung cancer, and regular patients.

Paper	Method	Image Type	Covid-19 Vs. Pneumonia Vs. Cancer Vs. Normal				
			ACC.(%)	SEN. (Recall)(%)	SPC.(%)	Pre.(%)	F1 –Score (%)
Celik [39]	CovidDWNet+GB	X-ray	96.81	-	-	-	-
		X-ray + CT	96.32	-	-	-	-
Alshmrani, et al.[40]	VGG19 + CNN	X-ray	96.48	93.75	-	97.56	95.62
Malik and Anees [41]	ResNet-50	X-ray	97.15	98.30	-	98.50	98.83
Malik and Anees [41]	Vgg-19	X-ray	96.14	95.76	-	98.20	96.29
Ibrahim et al. [42]	ResNet152V2	X-ray + CT	95.31	95.31	98.4	-	95.31
Malik and Anees [41]	Inceptionv3	X-ray	95.10	95.80	-	96.66	98.83
Ibrahim et al. [42]	ResNet152V2+GRU	X-ray + CT	96.09	96.09	98.7	-	96.09
Ibrahim et al. [42]	ResNet152V2+Bi-GRU	X-ray + CT	93.36	93.16	97.8	-	93.26
Proposed Methodology	(DFC) + Pathing + Alex Net	X-ray	97.95	97.17	99.02	97.41	97.27
		Fusion (CT+X-ray)	98.47	98.44	99.46	98.54	98.48

Celik et al. [39] used the CovidDWNet+GB algorithm on X-ray images and achieved 96.81% accuracy, and 96.32% accuracy in the dataset containing X-ray and CT images

Alshmrani et al. [40] used VGG19 + CNN architecture on X-ray images and achieved 96.48 accuracies.

Malik et al. [41] used ResNet-50 on X-ray images and achieved 97.15% accuracy, used Vgg-19 on X-ray images achieving 96.14% accuracy, and used ResNet152V2 on X-ray and CT images together and performed 95.31% accuracy, used Inceptionv3 on X-ray images and achieve 95.10% accuracy.

Ibrahim et al. [42] used ResNet152V2+GRU on X-ray and CT images together and achieved 96.09% accuracy, and they used ResNet152V2+Bi-GRU on X-ray and CT images together and achieved 93.36% accuracy.

While the proposed model achieves higher accuracy than these previous models, that is, when using X-ray images only, it achieves 97.95% accuracy; when using X-ray and CT images together, it achieves 97.95% accuracy. In addition, the same data used in this paper [39-42] were used as a part of the data used in the proposed paper, whether it is a specific type of image (X-ray Or CT) or two types together.

4. conclusion

In this paper, a proposed deep CNN method that uses just one learning procedure to identify COVID-19 at an early stage, which leads to the possibility of avoiding the risks of death due to this virus and misdiagnosis, which leads to choosing the incorrect treatment using chest X-ray and CT images. This approach differs significantly from other efforts that use various images type in one learning process, these images are collected from different sources, and this group of images was not used with each other in any previous study. Firstly, every patch was learned from different types of images and different kinds of lung diseases using a separate CNN. Then, the available features are combined for each image and disease. Finally, all the multimodal learned features are fused by DFC to Perform the Softmax Classifier for diagnosing COVID-19 from other lung diseases. The practical outcomes indicate that the proposed model outperformed other existing works with 98.47 % accuracy.

5. Future works

As a future study, using other types of images such as PET and MRI with CT and X-ray in the datasets, lengthening the epochs, and utilizing different architectures like GAN for classification and augmentation improves the proposed model's performance. Taking into consideration the Public media data would be used to forecast illness cases and inform timely responses.

Author Contributions

1st author's contributions are as follows: The idea of the paper, methodology, applications, confirmation, written evaluation, research, resources, data gathering, preparing the first copy while writing, composing, editing, and reviewing. The 2nd and third authors have done the visualization, supervision, editing, reviewing, and project administration.

Declaration of Competing Interest

The authors declare that they have no known competing financial interests or personal relationships that could have appeared to influence the work reported in this paper.

References

1. Albahli, S.J.I.j.o.m.s., Efficient GAN-based Chest Radiographs (CXR) augmentation to diagnose coronavirus disease pneumonia. 2020. **17**(10): p. 1439.
2. WHO. Coronavirus (COVID-19)dashboard https://COVID19.who.int/. Accessed 10 May 2023.
3. Yan, L. et al., A machine learning-based model for survival prediction in patients with severe COVID-19 infection. 2020.
4. Nasiri, H. and S.A. Alavi, A novel framework based on deep learning and ANOVA feature selection method for diagnosis of COVID-19 cases from chest X-ray images. Computational intelligence and neuroscience, 2022. **2022**.
5. Öztürk, Ş., U. Özkaya, and M. Barstuğan, Classification of Coronavirus (COVID-19) from X-ray and CT images using shrunken features. International Journal of Imaging Systems and Technology, 2021. **31**(1): p. 5-15.
6. Saha, P. and S. Neogy, Concat_CNN: A Model to Detect COVID-19 from Chest X-ray Images with Deep Learning. SN Computer Science, 2022. **3**(4): p. 1-11.
7. Bhargava, A., A. Bansal, and V. Goyal, Machine learning-based automatic detection of novel coronavirus (COVID-19) disease. Multimedia Tools and Applications, 2022. **81**(10): p. 13731-13750.
8. Absar, N., et al., Development of a computer-aided tool for detection of COVID-19 pneumonia from CXR images using machine learning algorithm. Journal of Radiation Research and Applied Sciences, 2022. **15**(1): p. 32-43.
9. Islam, M.R. and M. Nahiduzzaman, Complex features extraction with deep learning model for the detection of COVID19 from CT scan images using ensemble based machine learning approach. Expert Systems with Applications, 2022. **195**: p. 116554.
10. Shan, F., et al., Lung infection quantification of COVID-19 in CT images with deep learning. arXiv preprint arXiv:2003.04655, 2020.
11. Kogilavani, S., et al., COVID-19 Detection Based on Lung Ct Scan Using Deep Learning Techniques. Computational and Mathematical Methods in Medicine, 2022. **2022**.
12. Mishra, A.K., et al., Identifying COVID19 from chest CT images: a deep convolutional neural networks based approach. Journal of Healthcare Engineering, 2020. **2020**.
13. Rehman, N.-u., et al., A self-activated cnn approach for multi-class chest-related COVID-19 detection. Applied Sciences, 2021. **11**(19): p. 9023.
14. Aboughazala, L.M., Automated detection of COVID-19 coronavirus cases using deep neural networks with X-ray images. Al-Azhar University Journal of Virus Researches and Studies, 2020. **2**(1): p. 1-12.
15. Diaz-Escobar, J., et al., Deep-learning based detection of COVID-19 using lung ultrasound imagery. Plos one, 2021. **16**(8): p. e0255886.
16. Malik, H. and T. Anees, BDCNet: multi-classification convolutional neural network model for classification of COVID-19, pneumonia, and lung cancer from chest radiographs. Multimedia Systems, 2022: p. 1-15.
17. Rahman, M.M., et al., HOG+ CNN Net: Diagnosing COVID-19 and pneumonia by deep neural network from chest X-Ray images. Sn Computer Science, 2021. **2**(5): p. 1-15.
18. Sarkar, A., et al., Detection of COVID-19 from Chest X-rays using Deep Learning: Comparing COGNEX VisionPro Deep Learning 1.0TM Software with Open Source Convolutional Neural Networks. 2020.
19. Saood, A. and I. Hatem, COVID-19 lung CT image segmentation using deep learning methods: U-Net versus SegNet. BMC Medical Imaging, 2021. **21**(1): p. 1-10.
20. Hassantabar, S., M. Ahmadi, and A. Sharifi, Diagnosis and detection of infected tissue of COVID-19 patients based on lung X-ray image using convolutional neural network approaches. Chaos, Solitons & Fractals, 2020. **140**: p. 110170.
21. Imani, M., Automatic diagnosis of coronavirus (COVID-19) using shape and texture characteristics extracted from X-ray and CT-Scan images. Biomedical Signal Processing and Control, 2021. **68**: p. 102602.
22. Khalifa, N.E.M., et al., Detection of coronavirus (COVID-19) associated pneumonia based on generative adversarial networks and a fine-tuned deep transfer learning model using chest X-ray dataset. 2020.
23. Ibrahim, D.M., et al., Deep-chest: Multi-classification deep learning model for diagnosing COVID-19, pneumonia, and lung cancer chest diseases. 2021. **132**: p. 104348.
24. Xie, Y. and D. Richmond. Pre-training on grayscale imagenet improves medical image classification. in Proceedings of the European conference on computer vision (ECCV) workshops. 2018.
25. Bhandary, A., et al., Deep-learning framework to detect lung abnormality–A study with chest X-Ray and lung CT scan images. Pattern Recognition Letters, 2020. **129**: p. 271-278.
26. Cohen, J.P., et al., Covid-19 image data collection: Prospective predictions are the future. arXiv preprint arXiv:2006.11988, 2020.
27. P. Mooney, Chest x-ray images (pneumonia). https://www.kaggle.com/paultimot hymooney/chest-xray-pneumonia, 2020. (Accessed 17 December 2020.
28. Kermany, D.S., et al., Identifying medical diagnoses and treatable diseases by image-based deep learning. Cell, 2018. **172**(5): p. 1122-1131. e9.

29. Kireta, J., Unsupervised Dimension Reduction Techniques for Lung Cancer Diagnosis Based on Radiomics. 2023.
30. El Mansouri, O., Y. El Mourabit, and Y. El Habouz. System segmentation of Lungs in images chest x-ray using the generative adversarial network. in ITM Web of Conferences. 2022. EDP Sciences.
31. Ullah, N., et al., A Holistic Approach to Identify and Classify COVID-19 from Chest Radiographs, ECG, and CT-Scan Images Using ShuffleNet Convolutional Neural Network. Diagnostics, 2023. **13**(1): p. 162.
32. Sadik, F., et al., A dual-stage deep convolutional neural network for automatic diagnosis of COVID-19 and pneumonia from chest CT images. Computers in biology and medicine, 2022. **149**: p. 105806.
33. Gayathri, J., et al., A computer-aided diagnosis system for the classification of COVID-19 and non-COVID-19 pneumonia on chest X-ray images by integrating CNN with sparse autoencoder and feed forward neural network. Computers in biology and medicine, 2022. **141**: p. 105134.
34. Guoxin, W., et al., Bearing Fault Diagnosis Method Based on STFT Image and AlexNet Network, in Proceedings of TEPEN 2022: Efficiency and Performance Engineering Network. 2023, Springer. p. 1056-1068.
35. Minhas, R.A., et al., Shot classification of field sports videos using AlexNet Convolutional Neural Network. Applied Sciences, 2019. **9**(3): p. 483.
36. Zafar, A., et al., A Comparison of Pooling Methods for Convolutional Neural Networks. Applied Sciences, 2022. **12**(17): p. 8643.
37. Saad, W., et al., COVID-19 classification using deep feature concatenation technique. Journal of Ambient Intelligence and Humanized Computing, 2022: p. 1-19.
38. Rezazadeh, B., P. Asghari, and A.M. Rahmani, Computer-aided methods for combating Covid-19 in prevention, detection, and service provision approaches. Neural Computing and Applications, 2023: p. 1-40.
39. Celik, G., Detection of Covid-19 and other pneumonia cases from CT and X-ray chest images using deep learning based on feature reuse residual block and depthwise dilated convolutions neural network. Applied Soft Computing, 2023. **133**: p. 109906.
40. Alshmrani, G.M.M., et al., A deep learning architecture for multi-class lung diseases classification using chest X-ray (CXR) images. Alexandria Engineering Journal, 2023. **64**: p. 923-935.
41. Malik, H. and T. Anees, BDCNet: multi-classification convolutional neural network model for classification of COVID-19, pneumonia, and lung cancer from chest radiographs. Multimedia Systems, 2022. **28**(3): p. 815-829.
42. Ibrahim, D.M., N.M. Elshennawy, and A.M. Sarhan, Deep-chest: Multi-classification deep learning model for diagnosing COVID-19, pneumonia, and lung cancer chest diseases. Computers in biology and medicine, 2021. **132**: p. 104348.